DOI: 10.1002/cphc.200((will be filled in by the editorial staff))

Investigations of the Process Involved in the Borohydride Oxidation on La-Ni-Based Hydrogen Storage Alloys

Waldemir J. Paschoalino[a]; Stephen J. Thompson[b], Andrea E. Russell[b] and Edson A. Ticianelli *[a]

This work provides insights into the processes involved in the borohydride oxidation reaction (BOR) in alkaline media on metal hydride alloys formed by $LaNi_{4.7}Sn_{0.2}Cu_{0.1}$ and $LaNi_{4.78}Al_{0.22}$ with and without deposited Pt, Pd and Au. Results confirmed the occurrence of hydrolysis of borohydride ions when the materials are exposed to BH_4^- and a continuous hydriding of the alloys during BH_4^- oxidation measurements at low current densities; the activity for the direct BOR is low in both bare metal hydride alloys, but the rate of the BH_4^- hydrolysis and the hydrogen storage capacity are higher, while the rate of H diffusion is slower in the bare $LaNi_{4.78}Al_{0.22}$. Addition of Pt and Pd on both alloys resulted in an increase of the BH_4^- hydrolysis, but the H_2 formed is rapidly oxidized at the Pt modified catalysts. In the case of Au modification a small increase of the BH_4^- hydrolysis is observed, as compared to the bare alloys. The presence of Au and Pd also lead to a reduction of the rates of alloy hydriding/de-hydriding.

1. Introduction

High-energy density portable electricity generators are becoming of increasing importance. Direct borohydride fuel cells (DBFC) constitute an attractive class of renewable and sustainable energy sources that may help to meet these needs. However, there are some difficulties to be overcome to achieve full commercial implementation of such cells, including the need to improve the efficiency of the catalysts for the borohydride oxidation reaction (BOR) taking place in the DBFC anode. In alkaline media the BOR, can be promoted, liberating a maximum of 8 electrons and this main reaction is given in equation 1, below [1-3]:

$$BH_4^- + 8\ OH^- \rightarrow BO_2^- + 6\ H_2O + 8\ e^-\ (E^0 = -1.24\ V\ vs.\ ENH), \quad (1)$$

However, there are several parallel reactions that compete with the main reaction, diminishing the fuel utilization efficiency. These parallel reactions are the hydrolysis (equations 2 and 3) and the partial oxidation (equation 4) of the borohydride ions [1-4]:

$$BH_4^- + H_2O^- \rightarrow BH_3OH^- + 2\ H_{ads} \rightarrow BH_3OH^- + H_2 \quad (2)$$

$$BH_4^- + 2\ H_2O^- \rightarrow BO_2^- + 8\ H_{ads} \rightarrow BO_2^- + 4\ H_2 \quad (3)$$

$$BH_4^- + 4\ OH^- \rightarrow BO_2^- + 2\ H_2O + 4\ H_{ads} + 4\ e^- \rightarrow BO_2^- + 2\ H_2O + 2\ H_2 + 4\ e^- \quad (4)$$

Reaction (2) is predominant at low borohydride concentrations and reaction (3) at high concentrations. In the course of the BOR, the negative effect of hydrolysis may be reduced by the oxidation of the produced hydrogen in the working electrode:

$$H_2 \rightarrow 2\ H^+ + 2\ e^- \quad (5)$$

The borohydride oxidation reaction has been studied at a variety of materials, with the aim to prepare more efficient catalysts, and by employing a number of techniques, so to understand the reaction mechanisms. Hydrogen storage alloys formed by $LaNi_{4.7}Sn_{0.2}Cu_{0.1}$ with and without deposited Pt, $LaNi_{4.78}Al_{0.22}$, and $LaNi_{4.78}Mn_{0.22}$ have previously been investigated as electrocatalysts [5]. Evidence was found that wet exposure to sodium borohydride lead to the hydriding of the metal alloys, which were then capable of partially oxidizing the borohydride ions at same time during which the hydrogen produced by hydrolysis or partial oxidation of BH_4^- (reactions (2) - (3)) was being stored in the hydride form, that is,

$$MH_{ads} \rightarrow MH_{abs}, \quad (6)$$

[a] *W. J. Paschoalino, Prof. Dr. E. A. Ticianelli**
Instituto de Quimica de Sao Carlos, Universidade de Sao Paulo
Avenida Trabalhador Sancarlense, 400 Parque Arnold Schmidt, CP 780 13560-970, Sao Carlos, SP, Brazil
E-mail: edsont@iqsc.usp.br
[b] *S. J. Thompson, Prof. Dr. A. E. Russell*
Chemistry,University of Southampton,
Highfield Southampton, SO17 1BJ, UK
44 2380 593306
E-mail: a.e.russell@soton.ac.uk

As seen in previous work [5], the presence of platinum on the surface of $LaNi_{4.7}Sn_{0.2}Cu_{0.1}$ alloys provides a higher activity for the BOR, but at the same time the hydrolysis is more evident [5] when the electrode is at the open circuit potential. In spite of this, no hydrogen evolves from the electrode during anodic potential scans as any H_2 present is rapidly oxidized at the Pt sites.

The BOR has been extensively studied at Pt, Pd and Au catalyst surfaces [1-4,6-9].It has been found that Pd catalysts generally present similar behaviour as for Pt but with smaller involvement of the borohydride hydrolysis, whist for gold the occurrence of hydrolysis in very small although not negligible.

This work provides further insights into the processes involved in the borohydride oxidation reaction in alkaline media on metal hydride alloys, by investigating the reaction pathways of the BOR using *on line* mass spectrometry. Several metal hydride alloys were considered, including $LaNi_{4.7}Sn_{0.2}Cu_{0.1}$ and $LaNi_{4.78}Al_{0.22}$ at different electrode configurations, with and without deposition of platinum, palladium and gold. These alloys were chosen because of their reported high catalytic activity for the borohydride oxidation reaction, either directly or eventually involving a previous process of alloy hydriding [5,10]. The alloy with aluminium presents higher hydrogen storage capacity [10] compared to $LaNi_{4.7}Sn_{0.2}Cu_{0.1}$, but the hydrolysis pathways are higher more important than for $LaNi_{4.78}Al_{0.22}$ [5]. The deposition of the noble metals was made as an attempt to either modulate the participation of the borohydride hydrolysis or to contribute to the oxidation of the gaseous hydrogen evolved.

2. Results and Discussion

2.1. Physical and compositional characterization

The results obtained by EDS analyses confirmed, within the experimental errors, the alloy compositions given here by the metal alloy formulas. However, the noble metals (Pt, Pd and Au) could not be detected since there was a superposition of the EDS peaks with those of the other elements, which were present at much higher contents. Figure 1 shows the diffractograms obtained for the alloys with different compositions, with copper and tin or with aluminum. The results clearly show the formation of the metal hydride alloy of interest, as confirmed by the hexagonal $CaCu_5$-type features, characteristic of this type of material [11], and confirm the absence of segregated phases. However, also in these cases it was not possible to identify any characteristic fcc peak of Pt, Pd or Au, evidencing, as expected, the presence low amounts of these materials in the structure of the alloys particles. Figure 2 shows the TEM images for the $LaNi_{4.78}Al_{0.22}$ – Pd (Figure 2a) and $LaNi_{4.78}Al_{0.22}$ – Au (Figure 2b). It is possible to observe, for both compositions, the formation of a number of individual crystallites, present as planes of atoms with varying spatial orientations. Such features are characteristic of these types of metal alloys.

ICP-AES (Medac) was used to determine the noble metal loading of each of the modified catalysts and the results are presented in Table 1. These data indicate that the depositions resulted in a very low loading of the noble metals, in the range of 0.1 to 0.3 wt.%. Since the total loading of the materials in the TPC layer in the working electrodes are of the order of 1.5 mg and the geometric area is 0.196 cm^2, these results indicate a loading of 9 to 25 $\mu g\ cm^{-2}$ of the noble metal in the catalyst layer.

Cyclic voltammograms were obtained using TPC electrodes in 1.0 mol L^{-1} KOH solutions for the $LaNi_{4.7}Sn_{0.2}Cu_{0.1}$with and without the noble metals and the results are shown in Figure 3.

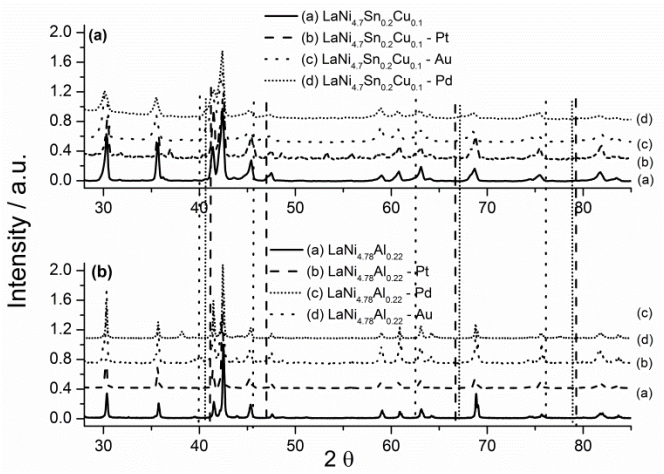

Figure 1. XRD features for the metal hydride alloys with and without deposited Pt, Pd and Au. Dashed, dotted and fine dotted lines are placed to localize the diffraction peaks of Pt, Au and Pd, respectively.

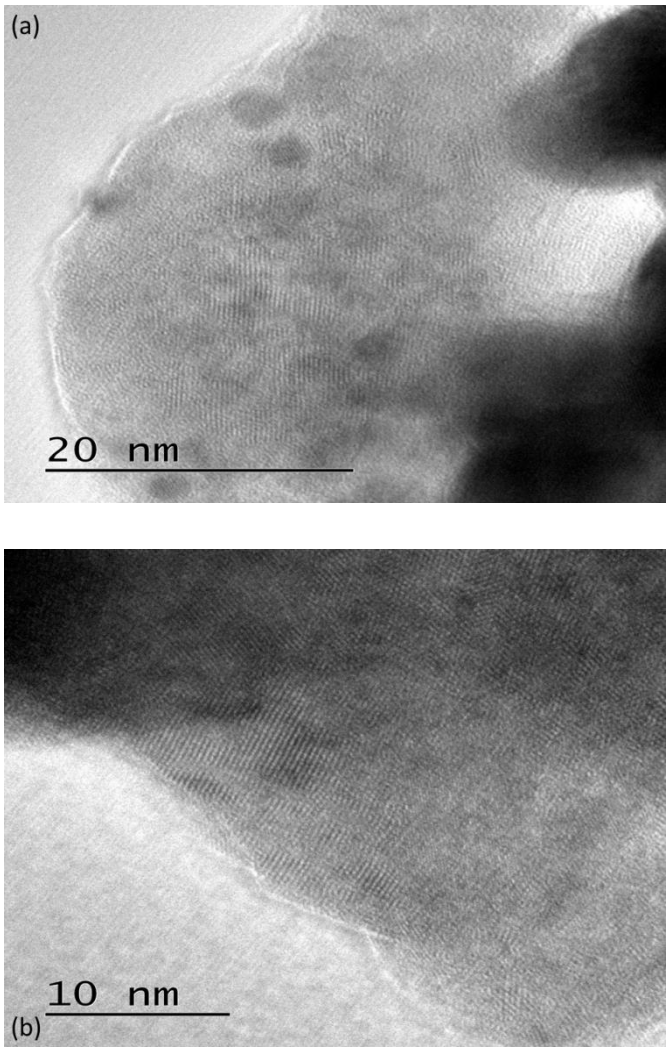

Figure 2. TEM of a $LaNi_{4.78}Al_{0.22}$ – Pd (a) and $LaNi_{4.78}Al_{0.22}$ – Au (b) alloy particles

Table 1 - Results of elemental analyses of the samples in weight percentage

Sample	Element	Composition (wt. %)
$LaNi_{4.7}Sn_{0.2}Cu_{0.1}$ – **Pt**	Pt	0.14
$LaNi_{4.7}Sn_{0.2}Cu_{0.1}$ – **Pd**	Pd	0.34
$LaNi_{4.7}Sn_{0.2}Cu_{0.1}$ – **Au**	Au	0.12
$LaNi_{4.78}Al_{0.22}$ – **Pt**	Pt	0.16
$LaNi_{4.78}Al_{0.22}$ – **Pd**	Pd	0.30
$LaNi_{4.78}Al_{0.22}$ – **Au**	Au	0.33

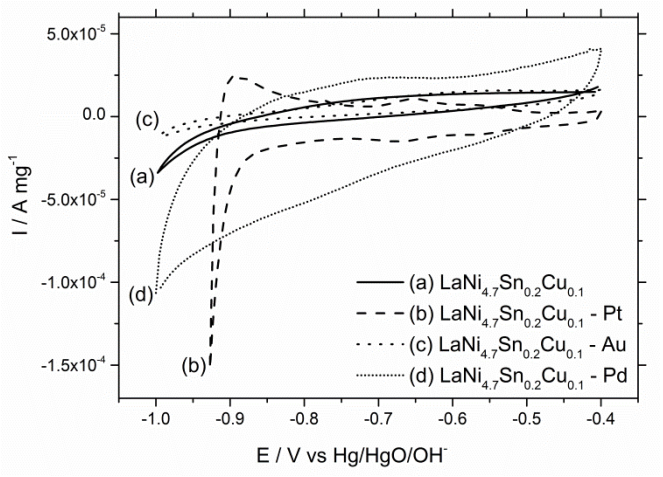

Figure 3. Cyclic voltammograms for TPC electrodes formed by the $LaNi_{4.7}Sn_{0.2}Cu_{0.1}$ alloy with and without Pt, Pd and Au in 1.0 M KOH solutions, v = 5 mV/s.

It is observed that there is an increase of the currents in the more negative potential regions of the cyclic voltammograms for the Pt-coated electrode, demonstrating an improvement of the electrocatalytic activity for the production/oxidation of adsorbed hydrogen, thus confirming the presence of Pt at the surface of the alloy particles [12]. Similar results were obtained when Pd was deposited in the alloy.

In contrast, for the gold containing particles there is no change of the hydrogen oxidation/reduction currents, consistent with the inactivity of the gold metal in this potential region. In summary, these results clearly evidence the presence of noble metals at the surface of the alloy particles, although no quantitative information regarding the surface area of the noble metal present could be obtained, given the broad features of the voltammograms and the need to limit the upper potential limit to -0.4 V (explained further, below), and therefore no correlations could be made with the quantitative data presented in Table 1.

2.2. Borohydride oxidation reaction

The polarization results of TPC rotating electrodes for $LaNi_{4.7}Sn_{0.2}Cu_{0.1}$ and $LaNi_{4.78}Al_{0.22}$ with and without Pt, Pd or Au, when BH_4^- ions were present in the solution, are shown in Figure 4. In these experiments the upper potential limit did not exceeded -0.4 V to avoid severe electrochemical oxidation of the metal hydride alloys. Particularly in the absence of Pt, Pd or Au for both group of alloys, the peak oxidation currents appearing in this range of potential do not evidence mass transport phenomena related to the presence of BH_4^- in the solution, so that the currents in Fig. 4 are not dependent on the rotation rate. This behavior has been attributed to the occurrence of the hydride oxidation reaction, for which the hydride formation is promoted by the hydrolysis of the borohydride ions [5]. In the presence of the noble metals, the direct oxidation of the borohydride ions is also evidenced by the increase of the currents at the more positive electrode potentials and their increase with the rotation rate, as illustrated in Fig. 4 with the results for $LaNi_{4.7}Sn_{0.2}Cu_{0.1}$ with Pt and $LaNi_{4.78}Al_{0.22}$ with Pd. Results also indicate that the magnitude of the hydride oxidation currents is strongly dependent on the metal hydride composition; this may be a consequence of the extension of the occurrence of the hydrolysis reaction of BH_4^- producing hydrogen or, more probably, of the rate of the hydriding process, leading to a smaller accumulation of hydrogen atoms inside the alloy structure after the deposition of the noble metal.

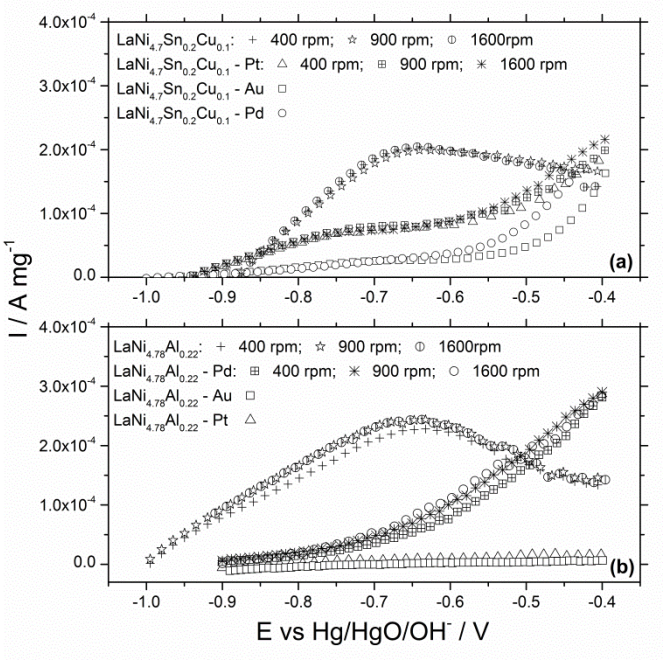

Figure 4. Polarization curves in 1.0 KOH with 10^{-2} M $NaBH_4$ for TPC rotating disc electrodes: (A) for $LaNi_{4.7}Sn_{0.2}Cu_{0.1}$ with and without Pt, Pd and Au; (B) for $LaNi_{4.78}Al_{0.22}$ with and without Pt, Pd and Au; at w = 1600 rpm v = 5 mV/s.

Figure 5 shows results of DEMS for the detection of H_2 for the electrodes at the open circuit potential (OCP), after the BH_4^- ions are added to the solution at t = 100-200 s. These results show that in all cases there is a release of H_2 as soon as the BH_4^- ions are introduced in the solution. However, for the bare $LaNi_{4.7}Sn_{0.2}Cu_{0.1}$ alloy and for that containing Au the evolution of H_2 is much less significant. It should be also noted that at the other extreme, for the $LaNi_{4.78}Al_{0.22}$ alloys, the DEMS signals for H_2 are much higher than for the $LaNi_{4.7}Sn_{0.2}Cu_{0.1}$-based materials. As all of these experiments were conducted at the OCP, these results evidence very clearly the occurrence of the hydrolysis of the BH_4^- ions, but in the case of the bare and Au coated $LaNi_{4.7}Sn_{0.2}Cu_{0.1}$ materials the extent of this reaction is much smaller. For the $LaNi_{4.78}Al_{0.22}$ alloy, as H_2 is released at the bare alloy it is difficult to separate the specific effects of the noble metals on the release of H_2.

The effects of the electrode potential are evidenced by the results in Figure 6. The top pictures (labeled a) show the oxidation currents of the BOR, while in the bottom ones (labeled b) are the lines representing the ionization currents measured by the MS detector, corresponding to the m/z mass = 2. For $LaNi_{4.7}Sn_{0.2}Cu_{0.1}$ (Fig. 6A) it is observed that there is some hydrogen evolution during the course of the BOR, but only at higher electrode potentials where some currents related to the oxidation process of BH_4^- are evidenced. This indicates the occurrence of a partial oxidation of borohydride ions (reaction 4), as already proposed for bulk nickel-based catalysts [13]. For $LaNi_{4.7}Sn_{0.2}Cu_{0.1}$ with Pt or Au, the evolution of H_2 stops as soon as lower potential limit is applied. Moreover, even when the electrode potential is scanned to less negative values, the hydrogen evolution remains inactive. The causes of these effects might be different for both alloys: in the case of the gold-coated alloy it must be related to the small rate of the hydrolysis of BH_4^-, while for the Pt-containing material it is probably related to the facile oxidation of H_2 catalyzed by Pt. These currents are not observed in the corresponding voltammogram because of insufficient sensitivity.

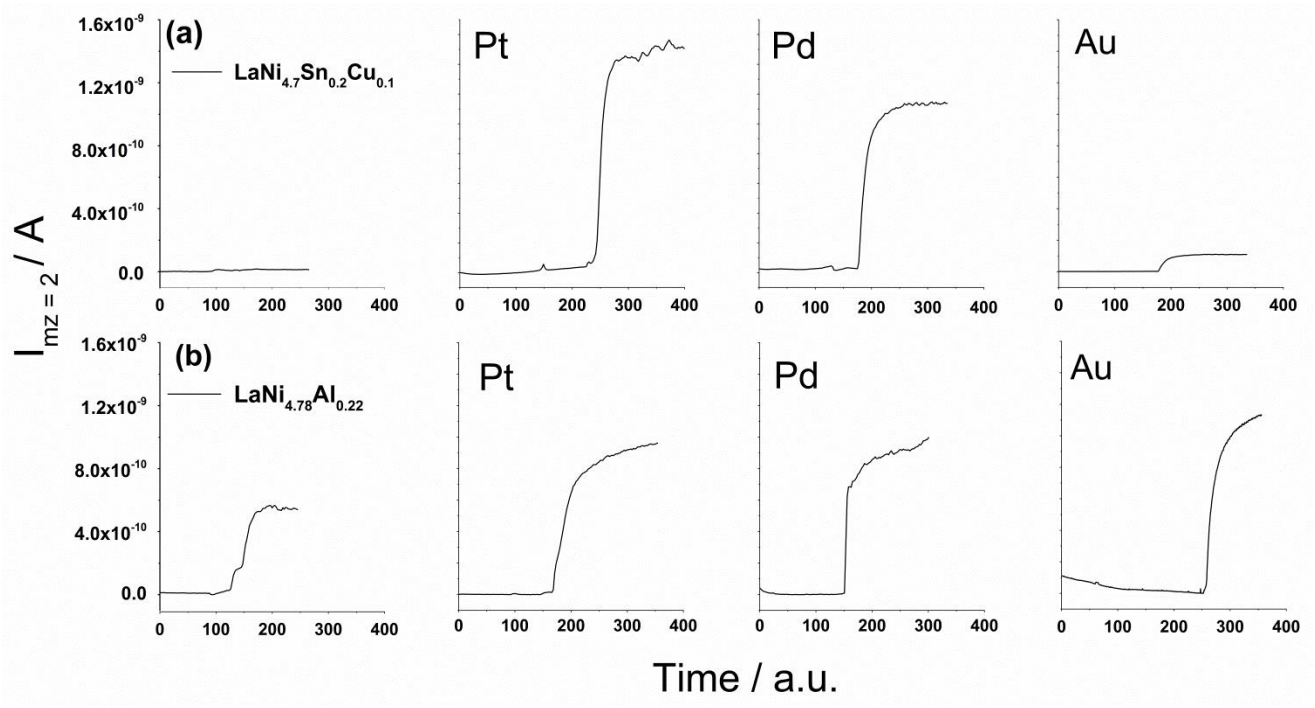

Figure 5. Mass spectrometry responses for H_2 detection for $LaNi_{4.7}Sn_{0.2}Cu_{0.1}$ and $LaNi_{4.78}Al_{0.22}$ without and with Pt, Pd and Au, in the presence of borohydride 10^{-2} M. Electrodes at the open-circuit potential.

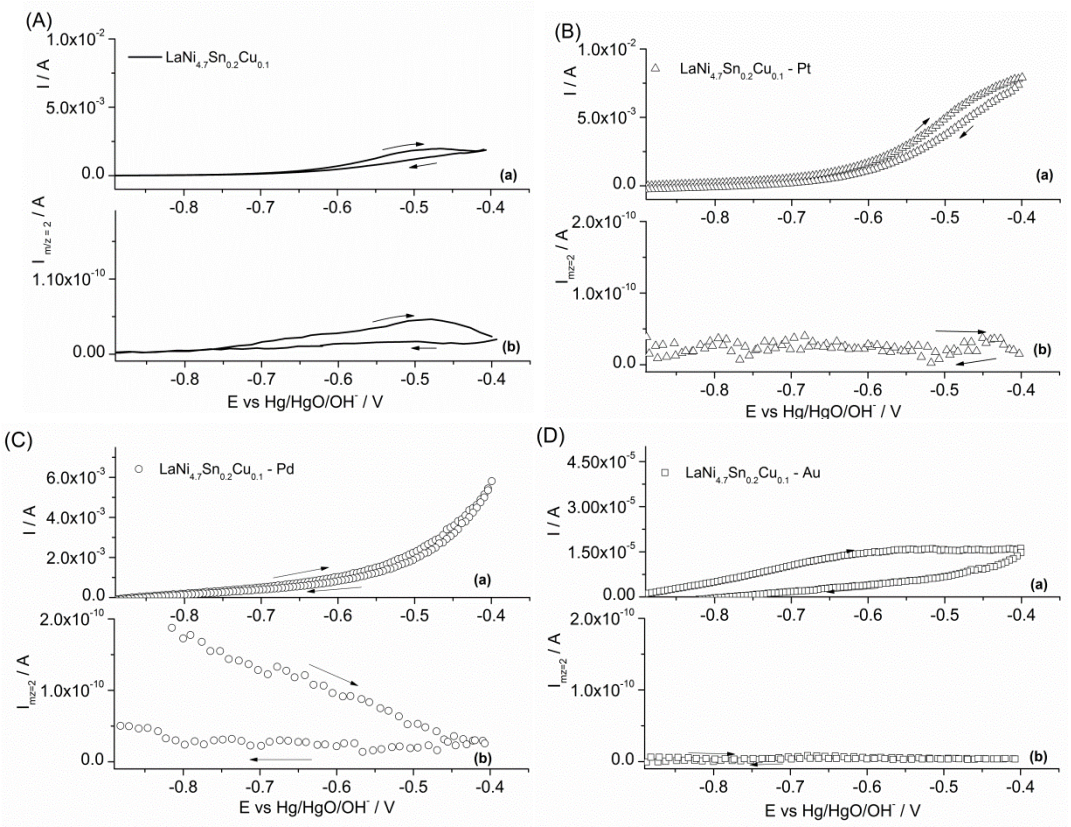

Figure 6. Online differential electrochemical mass spectrometry (DEMS) measurements for $LaNi_{4.7}Sn_{0.2}Cu_{0.1}$ with and without Pt, Pd and Au in the presence of borohydride 10^{-2} M: (a) voltammetric responses, (b) spectrometric responses for H_2 detection.

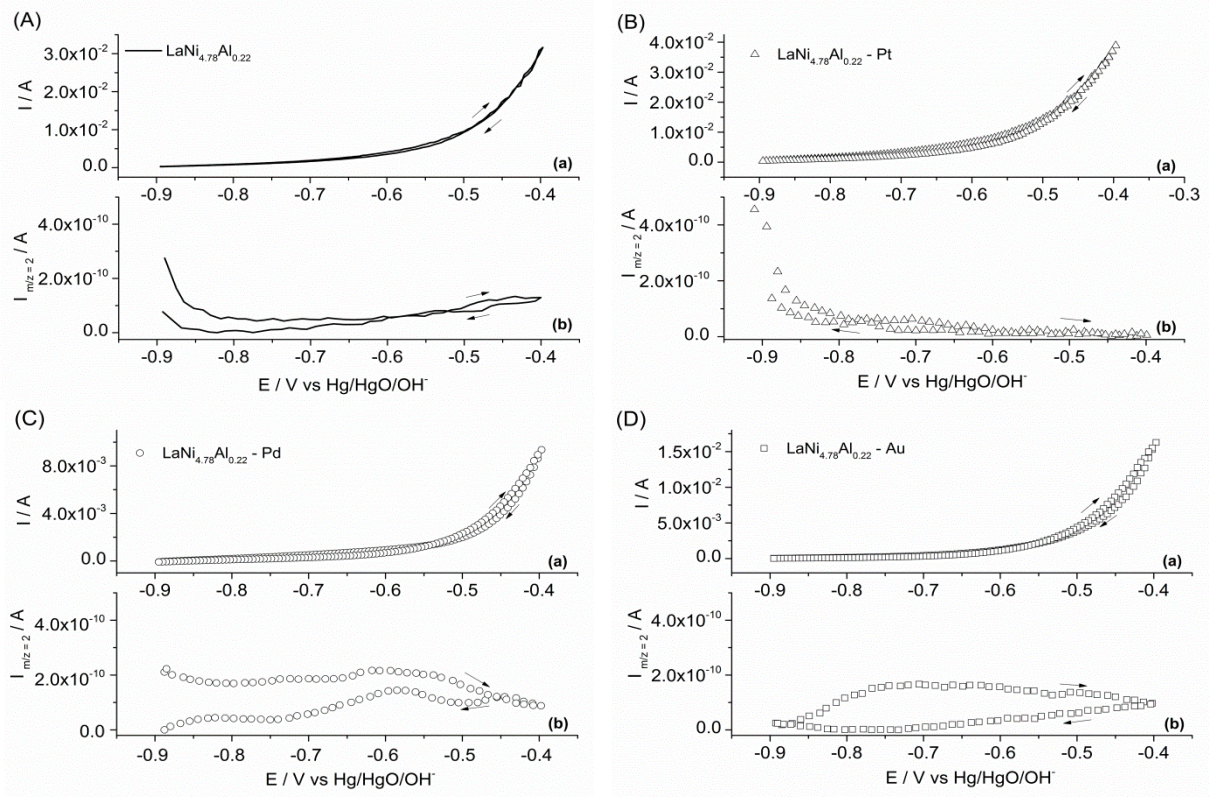

Figure 7. Online differential electrochemical mass spectrometry (DEMS) measurements for $LaNi_{4.78}Al_{0.22}$ with and without Pt, Pd and Au in the presence of borohydride 10^{-2} M: (a) voltammetric responses, (b) spectrometric responses for H_2 detection

When Pd is present, the DEMS results show a decrease in H_2 production with increasing electrode potential in the forward scan, while in the backward scan the hydrogen evolution remains inactive. These results suggest that there is some hydride accumulation inside the alloy before the beginning of the potential scan, which is then slowly but completely released along the forward scan. Here the rate of H_2 oxidation must be smaller than when Pt is present.

The results for the group of alloys based on $LaNi_{4.78}Al_{0.22}$ are shown in Figure 7. Here, a much greater release of H_2 is observed at the most negative potentials is observed for the alloy with and without Pt, evidencing a larger amount of BH_4^- hydrolysis. However in the course of the potential scan the hydrogen evolution diminishes rapidly indicating the BH_4^- hydrolysis stops and also that the BH_4^- partial oxidation reaction is not important. In the case of the Pt containing alloy, H_2 oxidation may also decrease the amount of H_2 detected by the DEMS measurements. The corresponding results for $LaNi_{4.78}Al_{0.22}$ with Pd or Au present are similar to those of $LaNi_{4.7}Sn_{0.2}Cu_{0.1}$ with Pd. That is, a decrease hydrogen evolution in the course of the potential scan is observed. However, here the suppression of the H_2 signal seems to be not total and this may be due to the larger rate of the BH_4^- hydrolysis.

Figure 8 shows galvanostatic discharge curves for $LaNi_{4.7}Sn_{0.2}Cu_{0.1}$ without and with Pt, Pd and Au for TPC electrodes electrochemically charged (Fig. 8a) and previously exposed to 10^{-2} M BH_4^- for 2 h, for electrolytes in the absence of dissolved BH_4^- (Fig 8b). Results for the $LaNi_{4.78}Al_{0.22}$ alloys previously exposed to 10^{-2} M BH_4^- for 2 h are shown in Figure 9. The time scales for the galvanostatic discharge curves reported were converted into discharge capacity (mA h g^{-1}) by multiplying by the time (*h*) for the discharge current (*mA*) and dividing by the alloy mass (*g*).

The discharge profiles in Fig. 8a for $LaNi_{4.7}Sn_{0.2}Cu_{0.1}$-based TPC electrodes show very similar characteristics to those reported for standard negative metal hydride electrodes of Nickel-metal hydride batteries, with some degradation of the maximum discharge capacity of the alloys observed after the incorporation of noble metals [5,11]. Interestingly, results for the alloys in Fig. 8b present essentially the same profiles as in Fig. 8a, confirming that all the materials are hydrided either electrochemically of by exposition to BH_4^- solutions. The lower maximum discharge capacities for the $LaNi_{4.78}Al_{0.22}$-based materials (Fig. 9), especially for the noble metal modified materials, is a consequence of the smaller alloy hydriding, as evidenced in Fig. 4b. This phenomenon can be attributed to the low diffusion rate of the H atoms inside the alloy. These results are consistent with the larger amount of H_2 released during the charging of the alloys, as observed in Fig. 6 for the $LaNi_{4.78}Al_{0.22}$-based materials, implying that the rates of the BH_4^- hydrolysis and H_2 release are greater than the rate of the hydrogen uptake by the alloy.

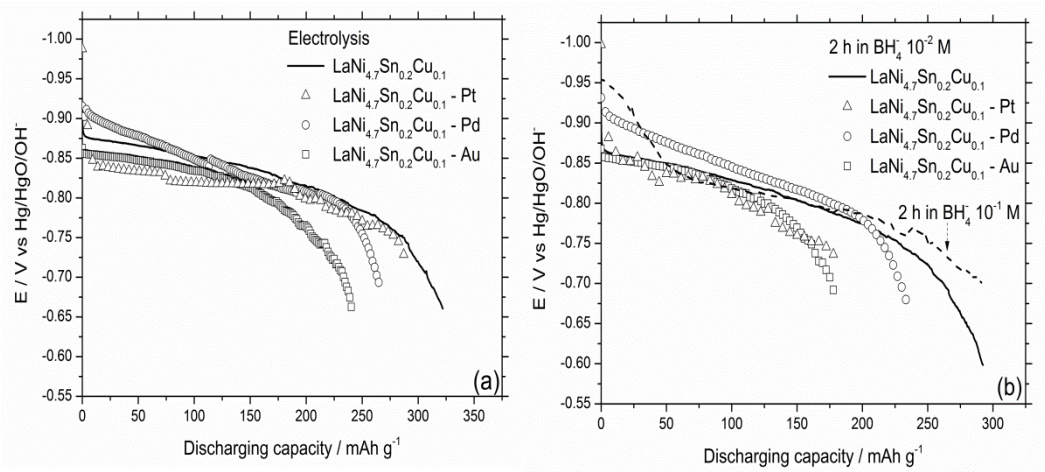

Figure 8. Galvanostatic discharge curves for $LaNi_{4.7}Sn_{0.2}Cu_{0.1}$ without and with Pt, Pd and Au. Two situations are considered: (a) electrode previously charged by electrolysis in 1.0 M KOH at 0.2 mA for 2 h; (b) electrodes previously exposed to $NaBH_4$ for 2 h, tested in the absence of $NaBH_4$ in the electrolyte.

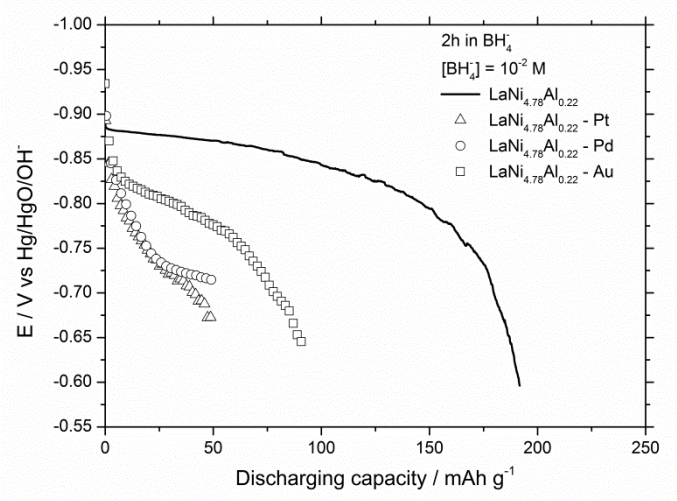

Figure 9. Galvanostatic discharge curves for $LaNi_{4.78}Al_{0.22}$ without and with Pt, Pd and Au with electrodes previously exposed to $NaBH_4$ for 2 h, tested in the absence of $NaBH_4$ in the electrolyte.

3. Conclusion

The present investigation shows that state of hydriding of $LaNi_{4.7}Sn_{0.2}Cu_{0.1}$ and $LaNi_{4.78}Al_{0.22}$ is important in defining the kinetics and outcome of the BOR at these materials. The extent of hydride formation has been shown to depend on the rate of the BH_4^- hydrolysis, the hydrogen storage capacity of the alloy, and kinetics of H atom diffusion inside the alloy. The activity for the direct BOR is low in both bare metal hydride alloys, but the rate of the BH_4^- hydrolysis and the hydrogen storage capacity are higher, while the rate of H diffusion is slower in the bare $LaNi_{4.78}Al_{0.22}$. Results have shown that both the bare and all the noble metal modified alloys can be hydrided either electrochemically or by exposure to BH_4^- solutions, although for the $LaNi_{4.78}Al_{0.22}$-based materials the extent of this phenomenon is smaller. A continuous hydriding of all $LaNi_{4.7}Sn_{0.2}Cu_{0.1}$-based and the bare $LaNi_{4.78}Al_{0.22}$ alloys are observed in the chronoamperometric BH_4^- oxidation measurements at low current densities. Addition of Pt on both alloys resulted in an increase of the BH_4^- hydrolysis, but the H_2 formed is rapidly oxidized, confirming the initial predictions for this noble metal. In addition, the rates of the alloy hydriding/de-hydriding were not significantly affected by the presence of Pt, but this was not the case for Pd and Au, for which there was a drastic reduction of the rate of these processes. In the case of gold some increase of the BH_4^- hydrolysis is observed, although its presence does not change significantly the performances of the bare alloys. All these phenomena point to the bare $LaNi_{4.7}Sn_{0.2}Cu_{0.1}$ as a more adequate alloy system for applications in DBFC/MH batteries.

Experimental Section

The $LaNi_{4.7}Sn_{0.2}Cu_{0.1}$ and $LaNi_{4.78}Al_{0.22}$ base alloys were prepared from high-purity metals by the arc melting technique under an inert gas atmosphere [11]. After that, the samples were gridded, and then a portion of these materials were separated and had the particle surfaces partially covered by a Pt, Pd or Au layers using galvanic displacement. This process involved the immersion of the metal hydride alloy in a 1.0 M of KOH solution containing 10^{-2} M of borohydride for two hours. After that, these materials were immersed in KOH 0.5 M solution containing 10^{-2} M of Pt or Pd or Au for more two hours.

Chemical and physical analyses of these materials were performed by energy dispersive spectroscopy (EDS) conducted using a scanning electron microscope (EDX LINK, Isis System Series with detector of SiLi pentafet, ATW II (Atmosphere Thin Window) with resolution 133 eV until 5.9 keV linked to electronic microscope ZEISS LEO 440) and X-ray diffraction (XRD) conducted using a Rigaku RU200B X-ray diffractometer with Cu K_α radiation source. Normal (TEM) images (JEOL JEM 2100) of the alloy particles were obtained so to characterize the alloy micro- and nano-structures. Elemental analyses were made for identifying the amount of Pt, Pd and Au in each sample. Elemental analysis (MEDAC LTD) were performed to confirm the noble metal loading in the materials

The working electrode was a thin porous coating (TPC) structure deposited on rotating glassy carbon disc substrate. The TPC layer was prepared using 300 mg of the alloy in 0.5 mL of Nafion 0.05 wt.%; 15 µL of this suspension was deposited on the rotating glassy carbon disc, which was then allowed to dry under ambient conditions [5].

The TPC working electrode was evaluated in a single compartment cell with a high surface area platinum screen counter electrode and an Hg/HgO/KOH 1.0 M reference electrode. The experiments were conducted in 1.0 mol L^{-1} KOH, in the absence or in the presence of sodium borohydride 10^{-2} or 10^{-1} mol L^{-1} as a reactant. Results were collected using cyclic voltammetry, galvanostatic chronopotentiometric discharge measurements, and *online* differential electrochemical mass spectrometry (DEMS). For the DEMS measurements, the setup consisted of a Pfeiffer Vacuum QMA 200 quadrupole mass spectrometer with two differential pumping chambers [14]. The mass spectrometry (MS) measurements were conducted in 1 M KOH + 10^{-2} M $NaBH_4$ solution and the m/z = 2 signal (the H_2 signature) was measured as a function of the electrode potential.

Acknowledgements

The authors acknowledge FAPESP (Fundação de Amparo a Pesquisa do Estado de Sao Paulo, Brazil processes number 2012/09109-2 and 2012/21835-0), for financial support. This research has been performed with the use of TEM facilities at the Research Complex at Harwell. The authors would like to thank the Research Complex for access and support to these facilities and equipment.

Keywords: La-Ni-based alloy; borohydride oxidation reaction; metal hydride alloy; galvanic displacement.

[1] F.H.B. Lima, A.M. Pasqualeti, M.B.M. Concha, M. Chatenet, E.A. Ticianelli, Electroch. Acta **2012**, 84 202–212.
[2] G. Lota, A. Sierczynska, I. Acznik, K. Lota, Int. J. Electrochem. Sci. **2014**, 9, 659-669.
[3] M. Chatenet, B. Molina Concha, G. Parrour, J. P. Diara, F.H. Lima , E. A. Ticianelli, U. B. Demirci, P. Miele (Eds.), Nova Science Publishers, Inc. **2011**, Ch. 5, 103-135.
[4] M. Chatenet, F. H. B. Lima, E. A. Ticianelli, J. Electrochem. Soc. **2010**, 157, B697-B704.
[5] W.J. Paschoalino, E.A. Ticianelli, Int. J. Hydrogen Energy **2013**, 38, 7344-7352.
[6] M. H. Atwan, E. I. Gyenge, D. O. Northwood, J. New. Mat Electrochem. System **2010**, 13, 21-27.
[7] A. Ignaszak, D. C. Kannangara, V. W. S. Lam, E. L. Gyenge, J. Electrochem. Soc. **2013**, 160, H47-H53.
[8] R. L. Arevalo, M. C. S. Escaño, F. Kasai, ACS Catal. **2013**, 3, 3031-3040.
[9] C. Ponce de Leon, F.C. Walsh, D. Pletcher, D.J. Browning, J.B. Lakeman, J. Power Sources **2006**, 155, 172-181.
{10] L. Wang, G. Wu, Z. Yang, Y. Gao, X. Mao, C. Ma. J. Mat. Sci. Tech. **2011**, 27(1), 46-50
[11] R. C. Ambrósio, E. A. Ticianelli J. Electrochem. Soc. **2003**, 50, 438-443
[12] F.H.B. Lima, J. Zhang, M.H. Shao, K. Sasaki, M.B. Vukmirovic, E.A. Ticianelli, R.R. Adzic, J. Phys. Chem. **2007**, 111, 404-410.
[13] B. H. Liu, Z.P. Li, S. Suda, Electrochim Acta **2004**, 49, 3097–3105.
[14] J. P. I Souza, S. L. Queiroz, F. C. Nart, Quim. Nova **2000**, 23, 384–391.

Received: ((will be filled in by the editorial staff))
Published online: ((will be filled in by the editorial staff))

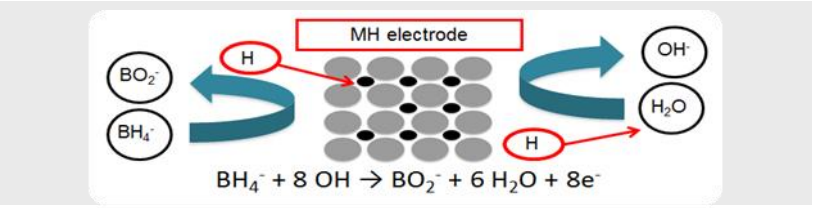

*Waldemir J. Paschoalino, Stephen J. Thompson, Prof. Dr. Andrea E. Russell and Prof. Dr. Edson A. Ticianelli**

Page No. – Page No.

Investigations of the Process Involved in the Borohydride Oxidation on La-Ni-Based Hydrogen Storage Alloys

Continuously chemically rechargeable metal hydride electrodes: insights for the understanding of the borohydride oxidation reaction in alkaline media are provided for metal hydride alloys formed by $LaNi_{4.7}Sn_{0.2}Cu_{0.1}$ and $LaNi_{4.78}Al_{0.22}$ chemically modified by platinum, palladium and gold deposits. Occurrence of hydrolysis of borohydride ions when the materials are exposed to BH_4^- and the continuous hydriding of the alloys are confirmed when the materials are exposed to BH_4^-.